Electrically tunable photonic true-time-delay line

Yuri O. Barmenkov[1]*, José Luis Cruz[2], Antonio Díez[2], Miguel V. Andrés[2]

[1]*Centro de Investigaciones en Óptica, Loma del Bosque 115, Col. Lomas del Campestre, 37150, León, Gto, México*
[2]*Departamento de Física Aplicada, Universidad de Valencia, Dr. Moliner 50, E46100 Burjassot (Valencia), Spain*
**yuri@cio.mx*

Abstract: We present a new application of the acousto-optic superlattice modulation of a fiber Bragg grating based on the dynamic phase and group delay properties of this fiber-optic component. We demonstrate a tunable photonic true-time-delay line based on the group delay change of the light reflected from the grating sidebands. The delay is electrically tuned by adjusting the voltage applied to a piezoelectric transducer that generates the acoustic wave propagating along the grating. In our experiments, a true-time delay of 400 ps is continuously adjusted (300 ps within the 3 dB amplitude range of the first sideband), using a 12 cm long uniform grating.

OCIS codes: (060.2340) Fiber optics components; (060.3735) Fiber Bragg gratings; (060.4080) Modulation; (230.1040) Acousto-optical devices; (350.4010) Microwaves.

References and links

1. J. Capmany, and D. Novak, "Microwave photonics combines two worlds," Nat. Photonics **1**(6), 319–330 (2007).
2. J. Yao, "Microwave Photonics," J. Lightwave Technol. **27**(3), 314–335 (2009).
3. C. Caucheteur, A. Mussot, S. Bette, A. Kudlinski, M. Douay, E. Louvergneaux, P. Mégret, M. Taki, and M. Gonz Lez-Herrāez, "All-fiber tunable optical delay line," Opt. Express **18**(3), 3093–3100 (2010).
4. Y. Liu, J. Yang, and J. Yao, "Continuous true-time-delay beamforming for phase array antenna using a tunable chirped fiber grating delay line," IEEE Photon. Technol. Lett. **14**(8), 1172–1174 (2002).
5. V. Italia, M. Pisco, S. Campopiano, A. Cusano, and A. Cutolo, "Chirped fiber Bragg gratings for electrically tunable time delay lines," IEEE J. Sel. Top. Quantum Electron. **11**(2), 408–416 (2005).
6. P. Perez-Millan, S. Torres-Peiro, J. Mora, A. Diez, J. L. Cruz, and M. V. Andres, "Electronic tuning of delay lines based on chirped fiber gratings for phased arrays powered by a single optical carrier," Opt. Commun. **238**(4-6), 277–280 (2004).
7. J. Capmany, B. Ortega, D. Pastor, and S. Sales, "Discrete-time optical processing of microwave signals," J. Lightwave Technol. **23**(2), 702–723 (2005).
8. X. Li, L. Peng, S. Wang, Y.-C. Kim, and J. Chen, "A novel kind of programmable 3^n feed-forward optical fiber true delay line based on SOA," Opt. Express **15**(25), 16760–16766 (2007).
9. A. Zadok, O. Raz, A. Eyal, and M. Tur, "Optically controlled low-distortion delay of GHz-wide radio-frequency signals using slow light in fibers," IEEE Photon. Technol. Lett. **19**(7), 462–464 (2007).
10. B. Ortega, J. L. Cruz, J. Capmany, M. V. Andrés, and D. Pastor, "Analysis of a microwave time delay line based on a perturbbed uniform fiber Bragg grating operating at constant wavelength," J. Lightwave Technol. **18**(3), 430–436 (2000).
11. L. Wei, W. Xue, Y. Chen, T. T. Alkeskjold, and A. Bjarklev, "Optically fed microwave true-time delay based on a compact liquid-crystal photonic-bandgap-fiber device," Opt. Lett. **34**(18), 2757–2759 (2009).
12. Z. Wang, K. S. Chiang, and Q. Liu, "Microwave photonic filter based on circulating a cladding mode in a fiber ring resonator," Opt. Lett. **35**(5), 769–771 (2010).
13. Y. Liu, J. Yao, and J. Yang, "Wideband true-time-delay beam former that employs a tunable chirped fiber grating prism," Appl. Opt. **42**(13), 2273–2277 (2003).
14. S. Blais, and J. Yao, "Photonic true-time delay beamforming based on superstructured fiber Bragg grating with linearly increasing equivalent chirps," J. Lightwave Technol. **27**(9), 1147–1154 (2009).
15. M. Delgado-Pinar, D. Zalvidea, A. Díez, P. Pérez-Millan, and M. V. Andrés, "Q-switching of an all-fiber laser by acousto-optic modulation of a fiber Bragg grating," Opt. Express **14**(3), 1106–1112 (2006).
16. W. F. Liu, P. St. J. Russell, and L. Dong, "Acousto-optic superlattice modulator using a fiber Bragg grating," Opt. Lett. **22**(19), 1515–1517 (1997).
17. P. St. J. Russell, and W. F. Liu, "Acousto-optic superlattice modulation in fiber Bragg gratings," J. Opt. Soc. Am. A **17**(8), 1421–1429 (2000).
18. C. Cuadrado-Laborde, A. Diez, M. Delgado-Pinar, J. L. Cruz, and M. V. Andrés, "Mode locking of an all-fiber laser by acousto-optic superlattice modulation," Opt. Lett. **34**(7), 1111–1113 (2009).
19. T. Erdogan, "Fiber grating spectra," J. Lightwave Technol. **15**(8), 1277–1294 (1997).
20. R. Kashyap, "Fiber Bragg Gratings," San Diego: Academic Press, 1999, chapter 4.

#128672 - $15.00 USD Received 18 May 2010; revised 8 Jul 2010; accepted 8 Jul 2010; published 4 Aug 2010

21. Y. O. Barmenkov, D. Zalvidea, S. Torres-Peiró, J. L. Cruz, and M. V. Andrés, "Effective length of short Fabry-Perot cavity formed by uniform fiber Bragg gratings," Opt. Express **14**(14), 6394–6399 (2006).

1. Introduction

Photonic true-time-delay (PTTD) lines attract much attention because of an increasing number of applications in microwave photonics [1,2] and communications [3]. Among these applications we can point out phased array antennas [4–6], microwave band-pass filters [7], buffering and packet synchronization [3,8]. The advantages of PTTD lines are their large bandwidth, high frequency operation and immunity to electromagnetic interference. In addition, fiber-based PTTD lines are readily compatible with fiber systems, robust, compact and lightweight, and they present low insertion loss.

In the framework of fiber-based PTTD lines, stimulated Brillouin scattering permits the implementation of optically controlled PTTD lines [9] which, in principle, have a potential fast time response, but with a relatively low delay time range (230 ps were reported using a fiber of 3.5 km length). Alternatively, tunable PTTD lines operated at a fixed optical carrier and based on an uniform or chirped FBGs perturbed by heating or mechanical stress [4,6,10] have found special attention due to their simple implementation and easy tuning. However, the time response of these thermally or mechanically controlled systems is below 1 ms.

Recently, some fiber-based PTTD lines that exploit novel approaches have been reported, although with severe limitations on the time delay range and time response (13 ps and 1 ms, respectively) [11] or the mechanical stability of the cladding modes [12].

There are a number of PTTD lines in which tunable light sources are required in order to adjust the time delay [13,14], but this approach cannot be implemented when a fixed optical carrier is required. In addition, the systems that require an array of tunable lasers are not easily scalable when a large number of independent delays need to be adjusted.

Our work is focused on the development of a tunable PTTD line with a fast response (in the μs range, see ref [15].), with a relatively large time delay range (400 ps), and operating with a fixed optical carrier. The solution that we report is based on the acousto-optic modulation of a uniform FBG, using a traveling longitudinal acoustic wave. Devices based on this interaction have been proposed as frequency shifters and tunable filters [16,17]. Recently, Q-switching and mode locking of all-fiber lasers have been demonstrated using FBG perturbed with a traveling and a standing acoustic wave, respectively [15,18]. In this paper, we show that the phase response properties of a uniform FBG modulated with an electrically-controlled acoustic wave permits the novel implementation of a tunable PTTD line.

2. Theoretical background

A longitudinal acoustic wave traveling along a uniform FBG written in a single-mode optical fiber induces a spatial sinusoidal phase modulation of the grating, which produces an effective sinusoidal chirp, moving synchronously with the acoustic wave. The phase modulation amplitude depends linearly on the acoustic wave amplitude [17]. Thus, the modal refractive index can be presented as

$$\begin{aligned} n(z,t) &= n_0 + n_1 \cos\left[Kz - \Delta\Phi \cos\left(k_s z + \Omega t\right)\right] = n_0 + n_1 J_0(\Delta\Phi)\cos\left(Kz\right) \\ &+2n_1 \cos\left(Kz\right)\sum_{m=1}^{\infty}(-1)^m J_{2m}(\Delta\Phi)\cos\left[2m\left(k_s z+\Omega t\right)\right] \\ &+2n_1 \sin\left(Kz\right)\sum_{m=1}^{\infty}(-1)^{m-1} J_{2m-1}(\Delta\Phi)\cos\left[\left(2m-1\right)\left(k_s z+\Omega t\right)\right], \end{aligned} \tag{1}$$

where n_0 is the effective index for LP_{01} mode, n_1 is the grating amplitude, $K = 2\pi/\Lambda$ is the unperturbed grating wavenumber (Λ is the grating period), z is a coordinate along the fiber, $\Delta\Phi$ is the phase modulation amplitude, k_s is the acoustic wavenumber, Ω is the angular acoustic frequency, m is a natural number, and J_m is the Bessel function of the m-th order. The probe light beam and the acoustic wave are chosen counter-propagating (see experimental

#128672 - $15.00 USD Received 18 May 2010; revised 8 Jul 2010; accepted 8 Jul 2010; published 4 Aug 2010

setup, Fig. 1). From Eq. (1) one can see that the longitudinal acoustic wave produces a series of traveling gratings with amplitudes depending on $\Delta\Phi$, which gives rise to a series of sidebands.

Using the coupled-wave theory [19,20], one can obtain the equations for two counter-propagating optical waves (one probe wave, $A_{\pm l}$, and one reflected wave, $B_{\pm l}$) falling into the $\pm l$-grating sideband and interacting with the grating described by Eq. (1):

$$\frac{dA_{\pm l}^{+}}{dz} = -i\Delta\beta_{\pm l}A_{\pm l}^{+} + i^{(l-1)}\kappa_l B_{\pm l}^{+} \tag{2a}$$

$$\frac{dB_{\pm l}^{+}}{dz} = i\Delta\beta_{\pm l}B_{\pm l}^{+} + (-i)^{(l-1)}\kappa_l A_{\pm l}^{+} \tag{2b}$$

where $\pm l$ is the sideband number, $A_{\pm l}^{+} = A_{\pm l}\exp\left(-i\Delta\beta_{\pm l}z\right)$, $B_{\pm l}^{+} = B_{\pm l}\exp\left(i\Delta\beta_{\pm l}z \pm il\Omega t\right)$, $\Delta\beta_{\pm l} = \beta - (\beta_0 \mp lk_s/2) = 2\pi n_0(\lambda^{-1} - \lambda_0^{-1}) \pm l\pi/\lambda_s$ is the detuning from the $\pm l$-sideband Bragg-wavelength, λ_0 is the Bragg wavelength of the unperturbed FBG, λ is the probe light wavelength, β and β_0 are the light wavenumbers that correspond to λ and λ_0, and $\kappa_l = \kappa J_l(\Delta\Phi)$ is the coupling coefficient for the l-th sideband (κ is the coupling coefficient of the unperturbed FBG). From Eqs. (2a) and (2b) one can easily obtain the complex reflectivity coefficient for the $\pm l$ sideband:

$$\rho_{\pm l} = \frac{-i^{\pm l}\kappa_{\pm l}\sinh\left(\gamma_{\pm l}L\right)}{\Delta\beta_{\pm l}\sinh\left(\gamma_{\pm l}L\right) + i\gamma_{\pm l}\cosh\left(\gamma_{\pm l}L\right)} \tag{3}$$

where $\gamma_{\pm l} = \sqrt{\left(\kappa_{\pm l}\right)^2 - \left(\Delta\beta_{\pm l}\right)^2}$ and L is the FBG length.

The spectrum of the FBG perturbed by a traveling acoustic longitudinal wave spreads to a number of sidebands with peak wavelengths (see also [16])

$$\lambda_{\pm l} = \lambda_0\left(1 \pm l\frac{\lambda_0}{2n_0\lambda_s}\right) \tag{4}$$

Thus, the positive sideband numbers correspond to longer wavelengths and *vice versa*. The optical frequency of the light reflected by the $\pm l$ sideband is shifted by $\mp lf_s$ in respect to the incident light frequency (f_s is the ultra-sound frequency).

The ensuing analysis is based on the theory developed in ref [21]. The group delay of the light reflected by the $\pm l$-sideband, $\tau_{\pm l}$, is found from the reflection coefficient phase:

$$\tau_{\pm l} = -\frac{\lambda^2}{2\pi c}\frac{d\phi_{\pm l}}{d\lambda}, \tag{5}$$

where $\varphi_{\pm l}$ is obtained from Eq. (3) as:

$$\phi_{\pm l} = -\mathrm{a}\tan\left[\left(\gamma_{\pm l}/\Delta\beta_{\pm l}\right)\mathrm{cotanh}\left(\gamma_{\pm l}L\right)\right] \tag{6}$$

Finally, the diffraction efficiency, $R_{\pm l}$, and the effective length of the $\pm l$-sideband, $L_{\pm l}^{eff}$, both at the sideband Bragg wavelength ($\Delta\beta_{\pm l} = 0$), and the final formula for the group delay are found:

$$R_{\pm l} = \left(\tanh\left(\kappa_{\pm l}L\right)\right)^2, \tag{7}$$

#128672 - $15.00 USD Received 18 May 2010; revised 8 Jul 2010; accepted 8 Jul 2010; published 4 Aug 2010

$$L_{\pm l}^{eff} = \frac{1}{2\kappa_{\pm l}} \tanh\left(\kappa_{\pm l} L\right) = \frac{L\sqrt{R_{\pm l}}}{2\mathrm{a}\tanh\left(\sqrt{R_{\pm l}}\right)}, \tag{8}$$

$$\tau_{\pm l} = 2n_0 L_{\pm l}^{eff} / c, \tag{9}$$

where $R_{\pm l} = \rho_{\pm l}\rho_{\pm l}^{*}$ (see Eq. (3)). From the last three formulae one can conclude that the sideband diffraction efficiency, the group delay and the effective length may be controlled by the amplitude of the phase modulation of the grating induced by the acoustic wave, which, in turn, depends on the acoustic wave magnitude. The sideband Bragg wavelength can be changed by adjusting the acoustical frequency within the PZT resonance in the case of a slight tuning, or by replacing the PZT with another one having the necessary resonance frequency. These features enable a number of new applications for these all-fiber tunable FBG-based devices that exploit the dynamic phase and group delay properties.

3. Experimental setup

The setup for the experimental characterization of the acousto-optic superlattice modulator (AOSLM) as a tunable PTTD line is shown in Fig. 1. Light from a single-frequency semiconductor laser (SL) modulated by an electro-optical amplitude modulator (EOM) with a frequency of f_m = 400 MHz is sent through the optical circulator to a long uniform FBG written in a standard photosensitive fiber; the radio-frequency (RF) modulation depth is chosen to be comparatively low (~10%), which maintains a practically linear regime of light modulation. The FBG is 12 cm long, with Bragg wavelength of 1530.8 nm and reflectivity of 99.99% (40 dB transmission attenuation at the Bragg wavelength) that corresponds to a coupling coefficient κ = 0.442 cm^{-1}.

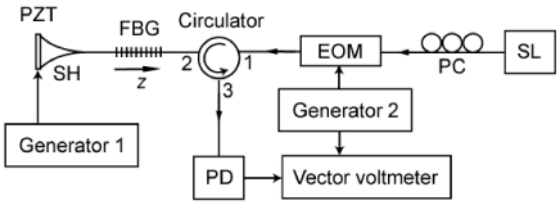

Fig. 1. Experimental setup. SL: semiconductor laser; PC: polarization controller; EOM: electro-optical amplitude modulator; FBG: fiber Bragg grating; PZT: piezo-electric transducer; SH: fused silica horn; PD: photodetector.

A longitudinal acoustic wave, generated by a piezoelectic (PZT) disk based on the P5H ceramic and attached to a heat sink, is launched along the FBG using a fused silica horn (SH). The PZT is driven by Generator 1 at the PZT resonance frequency (2.08 MHz). Light reflected from the FBG is measured by a photodetector connected to a vector voltmeter. AC voltage from Generator 2 drives the EOM, and is also used as a reference signal for the RF phase measurements.

4. Experimental results and discussion

First, we studied the diffraction efficiency of the FBG sidebands generated by the AOSLM. In this experiment a wide-spectrum LED was connected directly to the circulator port 1, and an optical spectrum analyzer (OSA) with a resolution of 20 pm to the port 3 (see Fig. 1), while Generator 2 was switched off. Figure 2a shows the FBG spectra at different AC voltages applied to the PZT. At low voltages, the ± 1 sidebands have amplitudes much higher than that of the high-order sidebands. Reflectivity of the ± 1 sidebands did not reach 100% because the OSA resolution was not enough to resolve comparatively narrow reflection peaks (3 dB spectrum width was measured to be ~40 pm). Note that a proper FBG design based on the grating apodization and chirping permits to increase the sideband width. When the FBG reflection spectrum was measured using an SL tuned to the sidebands' peaks, the maximum

#128672 - $15.00 USD Received 18 May 2010; revised 8 Jul 2010; accepted 8 Jul 2010; published 4 Aug 2010

reflectivity was ~98% (see Fig. 2b). In the experiment, the sideband efficiency was controlled within the 1%-error interval. The dependence of the + 1 sideband efficiency on the voltage applied to the PZT is in good agreement with Eq. (7), assuming that the amplitude of the phase modulation of the grating is proportional to the PZT voltage; a slight difference observed at high voltage amplitudes (> 4V) could be explained by a small heating of the PZT (less than 10°C), which slightly changes the PZT electromechanical coupling factor.

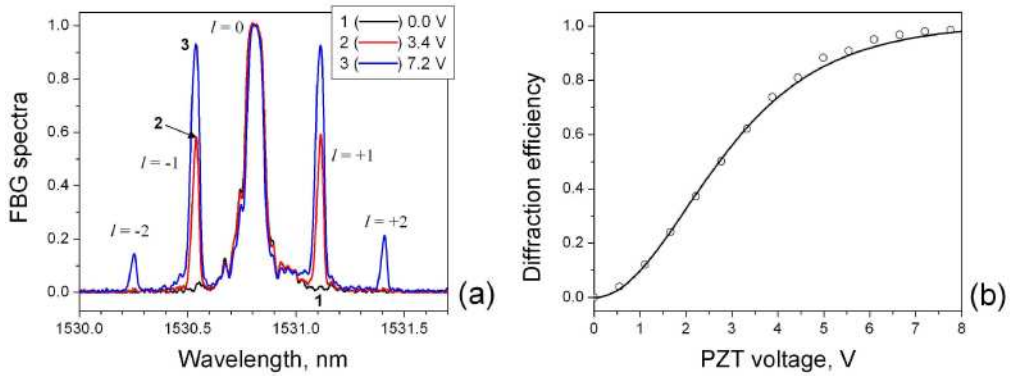

Fig. 2. (a) Spectra of FBG perturbed by ultra-sound wave at different PZT voltages (voltage's values are shown in the upper right corner); *l* indicates the sideband number. (b) Dependence of the + 1 sideband efficiency on PZT voltage. Circles: experimental data; solid line: fitting.

Second, we studied the dependence of the RF modulation envelope phase, Ψ_{+1}, for an optical carrier that matches the FBG's + 1 sideband, on the amplitude of the AC voltage applied to the PZT. The + 1 sideband was chosen for this study because it allows operation of AOSLM at low PZT voltages in comparison with high-order sidebands. The −1 sideband has the same properties as the + 1 sideband.

Ψ_{+1} is related directly to the + 1 sideband group delay τ_{+1} and the effective length L_{+1}^{eff}:

$$\Psi_{+1} = 2\pi\tau_{+1}f_m = 4\pi n_0 L_{+1}^{eff} f_m / c \qquad (10)$$

Thus, the dependence of Ψ_{+1} on + 1-sideband efficiency is the basic feature that permits to implement a dynamic control of the group delay and the effective length of the grating by means of the AC voltage.

Figure 3,a shows the experimental relationship between Ψ_{+1} and the amplitude of the AC voltage applied to the PZT. One can see that the phase decreases as voltage amplitude increases, which corresponds to a reduction of both the group delay and the effective length. Figure 3b plots these two parameters versus the + 1 sideband diffraction efficiency. The experimental data show a good agreement with Eqs. (8),(9). Since the optical path between the EOM and the photodetector was relatively long (the fiber length was ~2 m), producing an additional phase shift into the measured Ψ_{+1} values, the experimental data were corrected by a phase offset (the right scale in Fig. 3a) that permits to compensate the fiber length excess. The correcting parameter was chosen so that the + 1 sideband effective length is equal to a half of FBG physical length at low sideband efficiency (low PZT voltage), as the Eq. (8) predicts.

From Fig. 3b, one can conclude that the group delay and the effective length for the + 1 sideband strongly depend on its efficiency that is controlled electrically by AC voltage applied to the PZT. In our experiments, the group delay was adjustable from 150 ps to 550 ps, i.e., covering a range of 400 ps. Within the 3 dB range of the sideband efficiency, the group delay could be continuously adjusted from 150 to 450 ps (a range of 300 ps). The implementation of an automatic SL power control would permit to adjust the group delay at constant optical power, compensating for the reflectivity changes of the sideband.

#128672 - $15.00 USD Received 18 May 2010; revised 8 Jul 2010; accepted 8 Jul 2010; published 4 Aug 2010

The response time of this PTTD line is determined by the speed of the acoustic wave and the length of the grating, which gives a value of ~20 μs. This value is in good agreement with the response time obtained from the measurement of the sideband amplitude modulation [15].

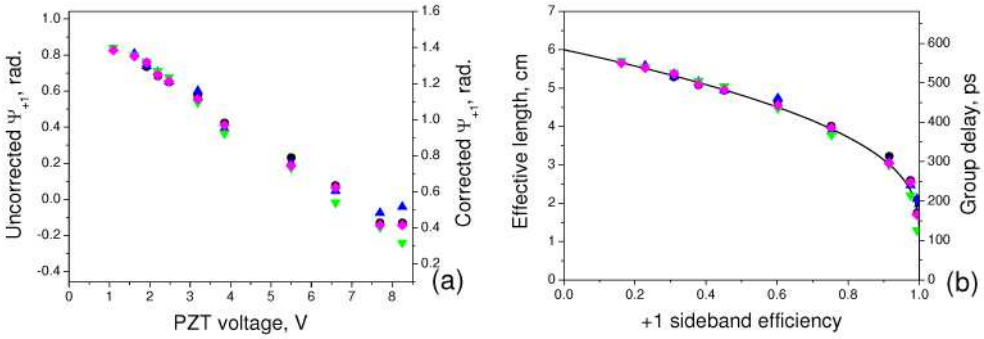

Fig. 3. (a) Dependence of the RF modulation envelope phase of light reflected from the FBG + 1 sideband on amplitude of voltage applied to PZT. The left scale: uncorrected values, the right scale: corrected values. (b) FBG + 1 sideband effective length and group delay versus the diffraction efficiency. Symbols: experimental data; solid line: curve calculated by Eq. (8). In both figures different symbols correspond to different experimental series.

5. Conclusion

In conclusion, we have carried out an experimental and theoretical study of the phase and group delay response of a FBG modulated by a longitudinal acoustic wave. The phase properties of the first sidebands permit the implementation of electrically-tuned PTTD line controlled by the AC voltage applied to the piezo-electric transducer that generates the acoustic wave. The proposed PTTD line permits to vary the group delay in the range of 400 picoseconds.

Acknowledgments

This work was supported by the Ministerio de Ciencia e Innovación of Spain (Grants No. PCI2005-A7-0209 and TEC2008-05490), and by the Generalitat Valenciana (Grant No. PROMETEO/2009/077).